

Band alignment in $\text{Ga}_x\text{In}_{1-x}\text{P}/\text{InP}$ heterostructures

A. Bensaada, J. T. Graham, J. L. Brebner, A. Chennouf, R. W. Cochrane, and R. Leonelli
*Département de Physique et Groupe de Recherche en Physique et Technologie des Couches Minces,
 Université de Montréal, Case Postale 6128, Succ. A, Montréal, Québec H3C 3J7, Canada*

R. A. Masut

*Département de Génie Physique et Groupe de Recherche en Physique et Technologie des Couches Minces,
 École Polytechnique, Case Postale 6079, Succ. A, Montréal, Québec H3C 3A7, Canada*

(Received 12 July 1993; accepted for publication 3 November 1993)

We report low temperature optical absorption measurements on $\text{Ga}_x\text{In}_{1-x}\text{P}/\text{InP}$ ($x < 0.2$) multiple quantum wells and strained-layer superlattices. The spectra show several well-defined peaks whose positions can be fitted within an envelope-function formalism including strain effects. We deduce conduction band offsets between the larger gap ternary and smaller gap binary materials ranging from 30 to 50 meV. Since these values are intermediate between the strain-induced shifts for the light- and heavy-hole valence bands, the electrons and heavy holes are localized in the InP layers (type I system), whereas the light holes have their quantum wells in the GaInP layers (type II system).

With the extensive development of multilayer semiconductor heterostructures for optoelectronics, considerable effort has been devoted to the theoretical and experimental investigation of band alignments. Reliable measurements of band offsets exist for a number of lattice-matched III-V heterostructures¹ but no experimental data are available for numerous lattice-mismatched systems, including $\text{Ga}_x\text{In}_{1-x}\text{P}/\text{InP}$ for $x \leq 0.2$. For this combination, the smaller gap material (InP) is unstrained while the larger gap one (GaInP) is under tension.

In this letter, we present a study of optical absorption in $\text{Ga}_x\text{In}_{1-x}\text{P}/\text{InP}$ ($x < 0.2$) multiple quantum wells (MQW) and strained layer superlattices (SLS) in order to determine their band alignment. The samples were grown at 640 °C by low pressure metal-organic chemical vapor deposition. Details of the growth procedure can be found in Ref. 2. Structural characterization was carried out through x-ray diffraction measurements using a Philips high resolution five-crystal diffractometer. After initial alignment, symmetric (004) and asymmetric (115) rocking curves were compared to numerically simulated spectra in order to determine the layer thickness, lattice parameters, and strains.² The structure of each sample is given in Table I.

The absorption measurements were performed at liquid helium temperatures using a Bomem DA3 Fourier transform spectrometer. Both SLS and MQW structures were grown

onto heavily ($n \approx 10^{19} \text{ cm}^{-3}$) sulfur-doped InP (001) substrates. Such heavy doping causes a large increase in the substrate absorption edge energy, which permits absorption measurements above the band gap of undoped InP without removal of the substrate under the heterostructure. A 250-Å-thick InP buffer layer was epitaxially grown before the heterostructures to block any sulfur diffusion.

The absorbances αl of our samples, normalized to the number of periods n , are shown in Fig. 1. Similar intensities are obtained in all samples for the main peak (A2), indicating that it arises from the heterostructure and not from the substrate or buffer layer. Its relatively small linewidth (full width at half-maximum $\sim 2\text{--}4 \text{ meV}$) is an indication of the excel-

TABLE I. Structural parameters for the $\text{Ga}_x\text{In}_{1-x}\text{P}/\text{InP}$ heterostructures. l : InP well thickness; l_b : GaInP barrier thickness; x : Ga concentration in the barrier; n : number of periods.

Sample	$l(\text{Å})$ ($\pm 5\%$)	$l_b(\text{Å})$ ($\pm 5\%$)	x (± 0.005)	n
CEM73S	84	84	0.124	25
CEM75S	84	87	0.105	7
CEM77S ^a	84	84	0.104	5
CFM97S	78	250	0.159	5
CFM98S	105	225	0.175	5

^aContains an additional 600-Å-thick $\text{Ga}_{0.07}\text{In}_{0.93}\text{P}$ layer between the InP buffer layer and the SLS.

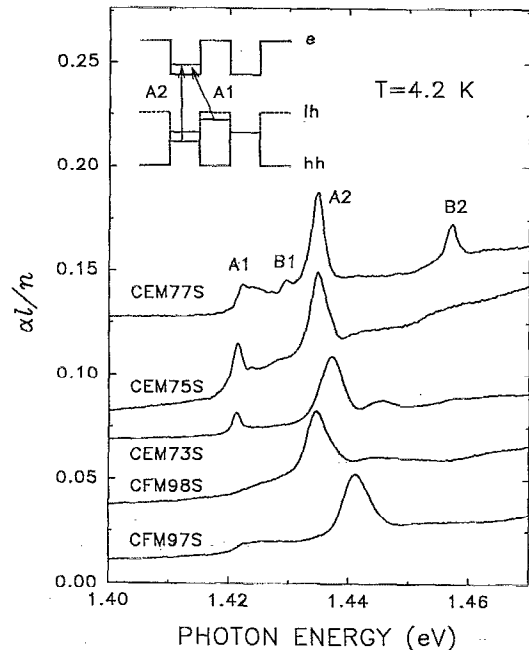


FIG. 1. Normalized absorbances for five GaInP/InP heterostructures. Each spectrum has been shifted for clarity. The inset schematizes the inferred band alignment.

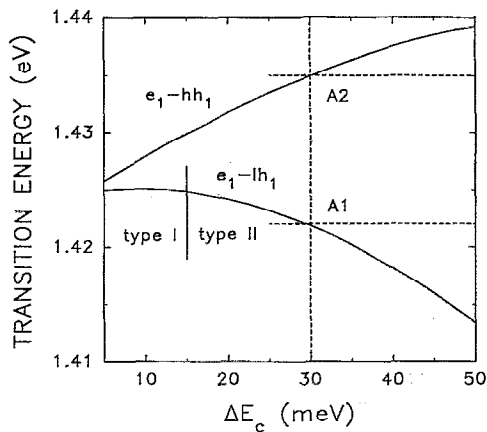


FIG. 2. Calculated energies of electron-light-hole (e_1 - lh_1) and electron-heavy-hole (e_1 - hh_1) transitions as a function of the conduction band offset using parameters appropriate for sample CEM77S. The experimental absorption peak energies are indicated by the horizontal lines.

lent quality of the samples. Depending on the sample, another peak (A1) or an absorption edge can be observed in the range 1.421–1.425 eV. Two additional peaks, B1 and B2, are observed in the absorption spectrum of sample CEM77S. They correspond to light-hole- and heavy-hole-conduction band transitions³ in the 600-Å-thick $\text{Ga}_{0.07}\text{In}_{0.93}\text{P}$ buffer layer which was added between the InP buffer layer and the SLS in this sample only. It can be seen that peak A2 is several times stronger than peak B2 even though the total InP well thickness is smaller than that of the GaInP buffer. This is indicative of a confinement-induced enhancement of the oscillator strength of the transition that gives rise to peak A2. It is worth noting that the A2 peak intensity corresponds to an absorption probability of 4×10^{-2} per layer, compared to around 6×10^{-3} per layer for transitions in AlGaAs/GaAs or 1.4×10^{-2} in GaInAs/AlInAs MQWs.^{4,5}

In order to identify the transitions at the origin of the structures observed in Fig. 1, we have used an envelope-function formalism⁶ with the strain effects included to calculate the energies of the electron and hole levels in the heterostructures. In the ternary layer, the tensile strain increases with the Ga concentration. This strain splits the degenerate Γ_8 valence band and shifts both the valence and conduction bands.⁷ Because the ternary layer is under tension, its light-hole band moves above the heavy-hole one and determines the band gap of the strained GaInP.^{3,8} The effects of confinement were calculated using the band structure of the strained GaInP layers (listed for each sample in Table II) and $E_g^{\text{InP}} = 1.423$ eV. The bulk effective masses were assumed to be the same in InP and GaInP: $m_e^* = 0.079$, $m_{lh}^* = 0.12$, and $m_{hh}^* = 0.65$.

Since the multilayer structural parameters have been independently determined, the only adjustable parameter in the model is the conduction band offset $\Delta E_c = E_c^{\text{GaInP}} - E_c^{\text{InP}}$. Figure 2 shows the electron-light-hole (e_1 - lh_1) and electron-heavy-hole (e_1 - hh_1) transition energies calculated as a function of the conduction band offset using parameters applicable to sample CEM77S. An offset of 30 meV gives an excellent fit to both A1 and A2 peaks if an exciton binding

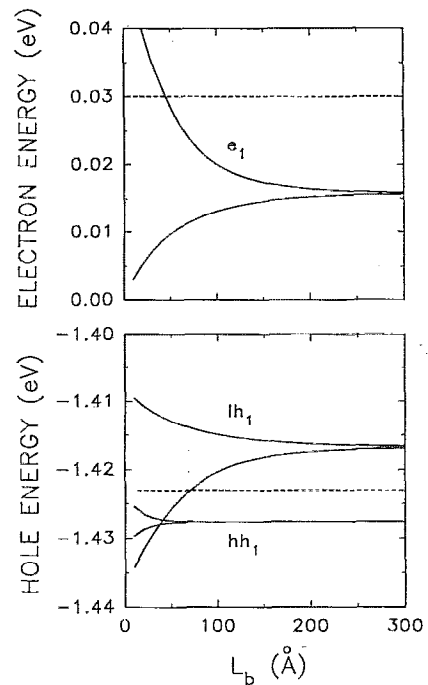


FIG. 3. Allowed energy bands for electrons (e_1), light holes (lh_1), and heavy holes (hh_1) as a function of the GaInP barrier thickness l_b . The energy scale is relative to the InP conduction band. The calculations were carried out assuming an InP well thickness $l = 84$ Å and a barrier Ga concentration $x = 0.104$. The dotted lines give the positions at which the states become unconfined.

energy E_B of 5 meV (the same as in bulk InP) is assumed for both transitions. Surprisingly, this value implies that the e_1 - lh_1 transition is of type II, i.e., the light holes and electrons are confined in the ternary GaInP layers and in the binary InP layers, respectively; the e_1 - hh_1 transition is of type I within the binary InP layers. This unusual band alignment is schematized by the inset in Fig. 1.

Figure 3 shows the allowed energy bands for electrons (e_1), light holes (lh_1), and heavy holes (hh_1) as a function of the GaInP barrier thickness l_b . For the samples where peak A1 can be observed, $l_b \approx 84$ Å, and the superlattice energy bandwidths span a significant fraction of the potential well for both electron and light-hole states. This explains the presence of a sharp e_1 - lh_1 transition in these samples: the delocalization of the electrons and light holes results in a strong overlap of the electron and hole wave functions, and thus in significant excitonic effects.⁹ For samples CFM97S and CFM98S, $l_b > 225$ Å and the resulting structures are MQWs. In this case, electrons and light holes are spatially separated and only an absorption edge is expected at the e_1 - lh_1 transition energy.

The values of ΔE_c for samples CEM73S and CEM75S were adjusted to match the e_1 - lh_1 transition energy to peak A1, assuming an exciton binding energy $E_B^{\text{lh}} = 5$ meV. Those for samples CFM97S and CFM98S were adjusted so that the e_1 - lh_1 transition corresponds to the absorption edge with no excitonic effects. The calculated values for ΔE_c , together with those for ΔE_v^{lh} and ΔE_v^{hh} , are given in Table II. ΔE_c is in the range 30–50 meV and tends to increase with increasing Ga concentration in the barrier. The e_1 - hh_1 exciton binding

TABLE II. Strained GaInP lh- and hh-cb band gaps E_g^{lh} and E_g^{hh} at 4.2 K, and calculated conduction band offsets ΔE_c , valence band offsets ΔE_v^{lh} and ΔE_v^{hh} , and heavy-hole exciton binding energies E_B^{hh} for the samples studied in this work.

Sample	E_g^{lh} (eV)	E_g^{hh} (eV)	ΔE_c (meV)	ΔE_v^{lh} (meV)	ΔE_v^{hh} (meV)	E_B^{hh} (meV)
CEM73S	1.440	1.497	36	-19	38	5
CEM75S	1.438	1.485	32	-17	30	6
CEM77S	1.438	1.484	30	-15	31	5
CFM97S	1.444	1.519	47	-26	49	9
CFM98S	1.446	1.529	41	-18	65	8

energy E_B^{hh} , determined from the difference between the calculated e_1 -hh₁ band-to-band transition and peak A2, is also given in Table II. It can be seen that the stronger overlap of the electron-hole wave functions as the heterostructures change from SLS to MQW results in an increase of E_B^{hh} , as was also observed in the AlGaAs/GaAs system.¹⁰

In summary, the low temperature optical absorption spectra of GaInP/InP heterostructures are characterized by a very intense e_1 -hh₁ absorption peak while the e_1 -lh₁ transition is evidenced by a weaker peak in SLSs and an absorption edge in MQWs. Comparison between the experimental spectra and calculations based on the envelope-function model including strain effects leads to a band alignment such that the GaInP/InP heterostructures are of type II for the

electron-light-hole system and of type I for the electron-heavy-hole system.

This work was supported by the Natural Sciences and Engineering Research Council of Canada and by the Fonds pour la Formation de Chercheurs et l'Aide à la Recherche (Gouvernement du Québec). Two of the authors (A.B. and A.C.) acknowledge financial support from the Institute of Physics, University of Oran, Algeria. We thank R. Lacoursière and L. Isnard for their technical assistance.

- ¹ E. T. Yu, J. O. McCaldin, and T. C. McGill, in *Solid State Physics*, edited by H. Ehrenreich and D. Turnbull (Academic, Boston, 1992), Vol. 46, p. 1.
- ² A. Bensaada, R. W. Cochrane, and R. A. Masut, *Can. J. Phys.* **70**, 783 (1992).
- ³ A. Bensaada, A. Chennouf, R. W. Cochrane, R. Leonelli, P. Cova, and R. A. Masut, *J. Appl. Phys.* **71**, 1737 (1992).
- ⁴ P. Voisin, in *Heterojunctions and Semiconductor Superlattices*, edited by G. Allan, G. Bastard, N. Boccara, M. Laño, and M. Voos (Springer, Berlin, 1986), p. 79.
- ⁵ W. Stolz, J. C. Maan, M. Altarelli, L. Tapfer, and K. Ploog, *Phys. Rev. B* **36**, 4301 (1987).
- ⁶ G. Bastard, *Wave Mechanics Applied to Semiconductor Heterostructures* (Éditions de Physique, Les Ulis, 1988).
- ⁷ G. E. Pikus and G. L. Bir, *Sov. Phys. Solid State* **1**, 136 (1959); **1**, 1502 (1960).
- ⁸ A. Bensaada, R. W. Cochrane, R. A. Masut, R. Leonelli, and G. Kajrys, *J. Cryst. Growth* **130**, 433 (1993).
- ⁹ A. Chomette, B. Deveaud, F. Clérot, B. Lambert, and A. Regreny, *J. Lumin.* **44**, 265 (1989).
- ¹⁰ A. Chomette, B. Lambert, B. Deveaud, F. Clérot, A. Regreny, and G. Bastard, *Europhys. Lett.* **4**, 461 (1987).